Compact, Broad-Stopband Elliptic-Function Lowpass Filters Using Microstrip Stepped Impedance Hairpin Resonators

Lung-Hwa Hsieh and Kai Chang

Texas A&M University, Electrical Engineering Dept., College Station, TX 77843-3128, USA,
Tel.: 979-845-5285, *Fax*: 979-845-6259, *Email*: chang@ee.tamu.edu

***Abstract* — A compact elliptic-function lowpass filter is developed. Multiple cascaded microstrip hairpin resonators operated at different 3-dB cutoff frequencies are used to design the filter. The filters are evaluated by experiment and simulation with good agreement. The return loss is better than 12.84 dB from DC to 0.81 GHz. The insertion loss is less than 0.5 dB. The rejection is greater than 35.7 dB from 1.5 to 10 GHz. This compact, low loss, sharp cutoff frequency response, and broad stopband lowpass filter should be useful in many wireless communication systems.**

I. INTRODUCTION

Compact size and high performance microwave filters are highly demanded in many communication systems. Due to the advantages of small size and easy fabrication, the microstrip hairpin has been drawing much attention. From the conventional half-wavelength hairpin resonator to the latest stepped impedance hairpin resonator, a size reduction of the resonator has been dramatically achieved [1-4].

Small size lowpass filters are frequently required in many communication systems to suppress harmonics and spurious signals. The conventional stepped-impedance and Kuroda-identity-stubs lowpass filters only provide Butterworth and Chebyshev characteristics with a gradual cut-off frequency response. In order to have a sharp cut-off frequency response, these filters require more sections. Unfortunately, increasing the number of sections also increases the size of the filter and insertion loss. Recently, the lowpass filter using photonic bandgap and defect ground structures [5] illustrated good performance, but required a large space to implement. A compact semi-lumped lowpass filter was also proposed [6]. However, using lumped elements increase the fabrication difficulties.

The microstrip elliptic-function lowpass filters show the advantages of high performance, low cost and easy fabrication [7-9]. In [9], the elliptic-function lowpass filters using elementary rectangular structures provide a wide passband with a sharp cut-off frequency response, but a narrow stopband.

In this paper, an equivalent circuit model for the stepped impedance hairpin resonator is presented. Also, a compact elliptic-function lowpass filter using the stepped impedance hairpin resonator is demonstrated. The approximated dimensions of the lowpass filters are synthesized from the equivalent circuit model with the published element-value tables. The exact dimensions of the filter are optimized by EM simulation. The filter using multiple cascaded stepped impedance hairpin resonators operated at different 3-dB cutoff frequencies can provide a broad stopband. The measured results agree well with simulated results.

II. EQUIVALENT CIRCUIT MODEL FOR THE STEP IMPEDANCE HAIRPIN

The basic configuration of the stepped impedance hairpin resonator is shown in Fig. 1. The stepped impedance hairpin resonator consists of the single transmission line l_s and coupled lines with a length of l_c. Z_s is the characteristic impedance of the single transmission line l_s. Z_{oe} and Z_{oo} are the even- and odd-mode impedance of the symmetric capacitance-load parallel coupled lines with a length of l_c.

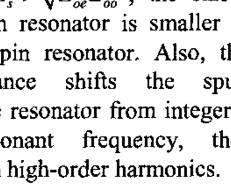

Fig. 1. Stepped impedance hairpin resonator.

By selecting $Z_s > \sqrt{Z_{oe}Z_{oo}}$, the size of the stepped impedance hairpin resonator is smaller than that of the conventional hairpin resonator. Also, the effect of the loading capacitance shifts the spurious resonant frequencies of the resonator from integer multiples of the fundamental resonant frequency, thereby reducing interferences from high-order harmonics.

The single transmission line is modeled as an equivalent L-C π-network as shown in Fig. 2(a). For the lossless

0-7803-7695-1/03/$17.00 © 2003 IEEE

2003 IEEE MTT-S Digest

single transmission line with a length of l_s, the *ABCD* matrix is given by

$$\begin{bmatrix} A & B \\ C & D \end{bmatrix} = \begin{bmatrix} \cos(\beta_s l_s) & jZ_s \sin(\beta_s l_s) \\ jY_s \sin(\beta_s l_s) & \cos(\beta_s l_s) \end{bmatrix} \quad (1)$$

where β_s and $Y_s=1/Z_s$ are the phase constant and characteristic admittance of the single transmission line, respectively. The *ABCD* matrix of the equivalent *L-C* π-network is

$$\begin{bmatrix} A & B \\ C & D \end{bmatrix} = \begin{bmatrix} 1+Z_L Y_c & Z_L \\ Y_c(2+Z_L Y_c) & 1+Z_L Y_c \end{bmatrix} \quad (2)$$

where $Z_L=j\omega L_s$, $Y_c=j\omega C_s$, w is the angular frequency, L_s and C_s are the equivalent inductance and capacitance of the single transmission line. Comparing equations (1) and (2), the equivalent L_s and C_s can be obtained as

$$L_s = Z_s \sin(\beta_s l_s)/\omega \quad \text{(H)} \quad (3a)$$

$$\text{and } C_s = [1-\cos(\beta_s l_s)]/[\omega Z_s \sin(\beta_s l_s)] \quad \text{(F)}. \quad (3b)$$

Moreover, as seen in Fig. 2(b), the symmetric parallel coupled lines are modeled as an equivalent capacitive π-network. The *ABCD* matrix of the lossless parallel coupled lines is expressed as [2]

$$\begin{bmatrix} A & B \\ C & D \end{bmatrix} = \begin{bmatrix} \dfrac{Z_{oe}+Z_{oo}}{Z_{oe}-Z_{oo}} & \dfrac{-j2Z_{oe}Z_{oo}\cot(\beta_c l_c)}{Z_{oe}-Z_{oo}} \\ \dfrac{j2}{(Z_{oe}-Z_{oo})\cot(\beta_c l_c)} & \dfrac{Z_{oe}+Z_{oo}}{Z_{oe}-Z_{oo}} \end{bmatrix} \quad (4)$$

where β_c is the phase constant of the coupled lines. Also, the *ABCD* matrix of the equivalent capacitive π-network is

$$\begin{bmatrix} A & B \\ C & D \end{bmatrix} = \begin{bmatrix} 1+Z_g Y_p & Z_g \\ Y_p(2+Z_g Y_p) & 1+Z_g Y_p \end{bmatrix} \quad (5)$$

where $Z_g=1/j\omega C_g$, $Y_p=j\omega C_p$. In comparison of equations (4) and (5), the equivalent capacitances of the p-network are found as

$$C_g = [Z_{oe}-Z_{oo}]/[2\,\omega Z_{oe} Z_{oo} \cot(\beta_s l_s)] \quad \text{(F)} \quad (6a)$$

$$\text{and } C_p = 1/[\omega Z_{oe} \cot(\beta_s l_s)] \quad \text{(F)}. \quad (6b)$$

Furthermore, combining the equivalent circuits of the single transmission line and coupled lines shown in Figures 2(a) and 2(b), the equivalent circuit of the stepped impedance hairpin resonator in terms of lumped elements *L* and *C* is shown in Fig. 2(c), where $C_{ps} = C_p+C_s+C_\Delta$ is the sum of the capacitances of the single transmission line, coupled lines and the junction discontinuity (C_Δ) between the single transmission line and the coupled lines. In addition, C_Δ can be expressed by [10]

$$C_\Delta \cong (0.012+0.0039\,\varepsilon_r)(w_c-w_s) \quad (6c)$$

where w_c is the width of the parallel-coupled lines and w_s the width of the single transmission line.

The approximated physical dimensions of the filter can be synthesized by using the available L-C tables [11] for filter design and equations (3) and (6). The widths of the single transmission line and coupled lines of the filter can be obtained from selecting the impedances that satisfy the condition $Z_s > \sqrt{Z_{oe}Z_{oo}}$. The lengths of the single transmission line and coupled lines of the filter transformed from (3a) and (6b) are

$$l_s = \sin^{-1}(\omega_c L_{st}/Z_s)/\beta_s \quad (7a)$$

$$\text{and } l_c = \tan^{-1}[\omega_c Z_{oe}(C_{pst}-C_s-C_\Delta)]/\beta_c \quad (7b)$$

where ω_c is the 3-dB cutoff angular frequency, L_{st} and C_{pst} are the inductance and capacitance chosen from the available L-C tables. C_s and C_g can be calculated from (3b), (7a) and (6a), (7b), respectively.

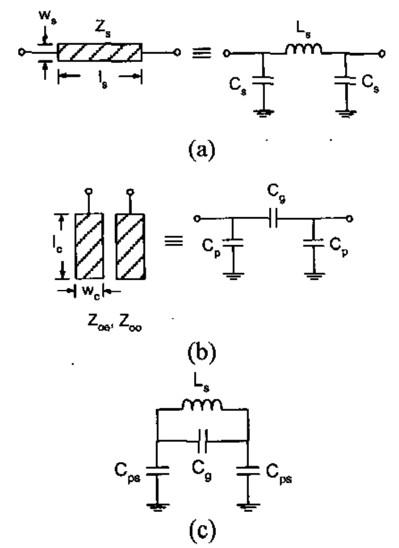

Fig. 2. Equivalent circuit of (a) single transmission line, (b) symmetric coupled lines, and (c) stepped impedance hairpin resonator by combining (a) and (b).

III. Broad Stopband Compact Elliptic-Function Lowpass Filters

The stopband of the elliptic-function filter using one stepped impedance hairpin resonator is limited by its harmonics, especially for its second harmonic [7]. To suppress the harmonics and to increase the stopband, additional resonators with a higher 3-dB cutoff frequency providing additional attenuation poles at harmonics can be added [8,12]. Fig. 3 shows different microstrip lowpass filters using different stepped impedance hairpin resonators designed at different 3-dB-cutoff frequencies, f_1, f_2, and f_3 GHz, respectively.

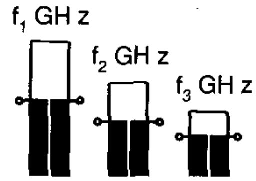

Fig. 3. The lowpass filters designed for f_1, f_2, and f_3 3-dB-cutoff frequencies.

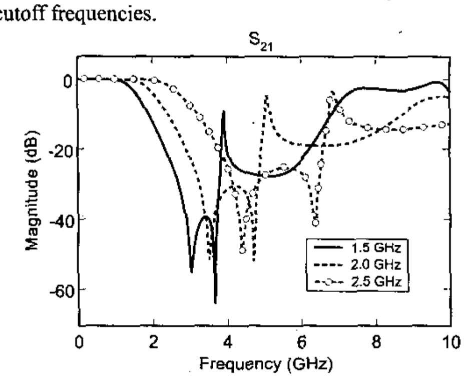

Fig. 4. Simulated results for the lowpass filters designed for 1.5, 2.0, 2.5 GHz 3-dB-cutoff frequencies.

Observing the simulated results in Fig. 4, the harmonics of the lower 3-dB-cutoff-frequency lowpass filters can be suppressed by using higher 3-dB-cutoff-frequency lowpass filters. The simulation was performed using EM simulation software IE3D [13]. To implement a broadband suppression at the stopband, a broad stopband lowpass filter using an adjacent transmission line to cascade any two resonators is shown in Fig. 5. The equivalent circuit of the filter is shown in Fig. 6.

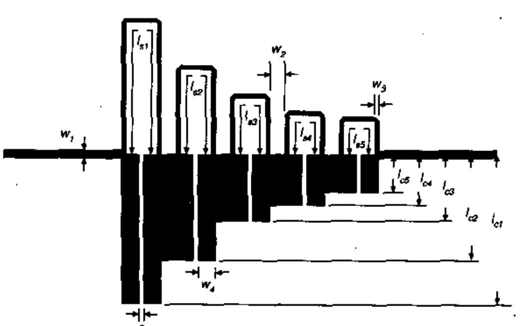

Fig. 5. Configuration of the broad stopband lowpass filter.

The resonators in the lowpass filter shown in Fig. 5 are designed at 1, 1.5, 2.2, 2.8 and 3.4 GHz 3dB-cutoff frequencies. In addition, using the available elliptic-function element-value tables [10] for filter design with impedance scaling, frequency scaling and selected impedances Z_s, Z_{oe}, Z_{oo} of the hairpin resonator, the approximated dimensions and L-C values of the lowpass filter can be synthesized by Eqs. (3), (6), (7) and (8).

$$C_{adj} = \varepsilon_o \, \varepsilon_r \, w_2 / h \qquad \text{(F/unit length)} \qquad (8)$$

where C_{adj} is the equivalent capacitance of the adjacent transmission line, w_2 is the width of the adjacent transmission line and h is the substrate thickness.

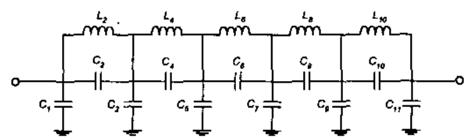

Fig. 6. Configuration of the broad stopband lowpass filter.

The filter using the available L-C values has a higher 3-dB cut-off frequency than designed one. This higher 3-dB cut-off frequency is due to the designed attenuation at the stopband of the lowpass filter [11]. To obtain the desired 3-dB cut-off frequency, the filter can be optimized by using an EM simulator [12] to tune the lengths of ls and lc of the hairpin resonator. The available, approximated and optimized L-C values of the filter using five cascaded hairpin resonators are listed in Table I. Also, the approximated and optimized dimensions of the filter are listed in Table II. The filter was fabricated on a 25mil thick RT/Duroid 6010.2 substrate with relative dielectric constant $\varepsilon_r = 10.2$.

TABLE I
L-C VALUES OF THE FILTER USING FIVE HAIRPIN RESONATORS

	C_1	L_2	C_2	C_3	L_4	C_4	C_5	L_6	C_6	C_7	L_8	C_8	C_9	L_{10}	C_{10}	C_{11}
Available L-C tables	2.87 pF	7.57 nH	0.6 pF	5.34 pF	5.05 nH	0.4 pF	3.6 pF	3.44 nH	0.27 pF	2.63 pF	2.7 nH	0.21 pF	2.11 pF	2.23 nH	0.18 pF	0.84 pF
Approximated L-C values	2.87 pF	7.57 nH	0.6 pF	5.34 pF	5.05 nH	0.39 pF	3.6 pF	3.44 nH	0.26 pF	2.63 pF	2.7 nH	0.2 pF	2.11 pF	2.23 nH	0.17 pF	0.84 pF
Optimized L-C Values	3.82 pF	10.24 nH	0.73 pF	7.25 pF	6.92 nH	0.52 pF	4.99 pF	4.86 nH	0.33 pF	3.55 pF	3.79 nH	0.25 pF	2.79 pF	3.24 nH	0.18 pF	1.14 pF

TABLE II
APPROXIMATED AND OPTIMIZED PHYSICAL DIMENSIONS OF THE FILTERS

	s	w_1	w_2	w_3	w_4	l_{s1}	l_{s2}	l_{s3}	l_{s4}	l_{s5}	l_{c1}	l_{c2}	l_{c3}	l_{c4}	l_{c5}
Approximated Dimensions	0.2 mm	0.56 mm	0.7 mm	0.2 mm	1.2 mm	13.23 mm	8.82 mm	6.02 mm	4.73 mm	3.89 mm	8.55 mm	5.63 mm	3.78 mm	2.93 mm	2.38 mm
Optimized Dimensions	0.2 mm	0.56 mm	0.7 mm	0.2 mm	1.2 mm	20.23 mm	13.82 mm	10.02 mm	7.73 mm	6.95 mm	10.05 mm	7.13 mm	4.53 mm	3.43 mm	2.59 mm

Fig. 7 shows the simulated results of the filters using approximated and optimized L-C values. Inspecting the simulated results, the filter using the approximated L-C values has a higher 3-dB cut-off frequency. Fig. 8 shows the measured and simulated results of the filter using the optimized L-C values. The lowpass filter has a 3-dB passband from DC to 0.96 GHz. The return loss is better than 12.84 dB from DC to 0.81 GHz. The insertion loss is less than 0.5 dB. The rejection is greater than 35.7 dB from 1.5 to 10 GHz. The ripple in the passband is +/- 0.25 dB.

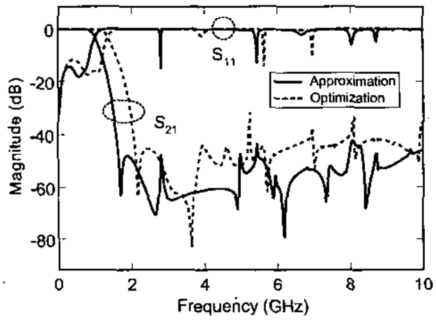

Fig. 7. Simulated results of the broad stopband lowpass filter with approximated and optimized dimensions.

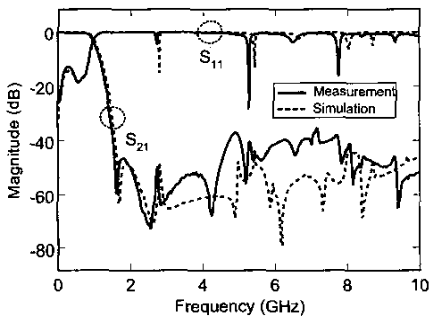

Fig. 8. Measured and simulated results of the broad stopband lowpass filter with optimized dimensions.

IV. Conclusion

A compact elliptic-function lowpass filter using stepped impedance hairpin resonators is proposed. The filter is synthesized from the equivalent lumped-element model using the available element-value tables. To obtain the desired 3-dB frequency, filters are optimized by an EM simulator. The lowpass filter using multiple cascaded stepped impedance hairpin resonators shows a broad stopband, a sharp cut-off frequency response, and low insertion loss. The measured results of the lowpass filter agree well with simulated results. This broad stopband compact elliptic-function lowpass filter is useful in many wireless communication systems.

Acknowledgement

The authors would like to thank Mr. Li of Texas A&M University for his technical assistance. This work was sponsored in part by NASA, Jet Propulsion Laboratory, and the TITF Program of Texas A&M University.

References

[1] J. S. Wong, "Microstrip tapped-line filter design," *IEEE Trans. Microwave Theory Tech.*, Vol. 27, No. 1, pp. 44-50, January 1979.

[2] M. Sagawa, K. Takahashi and M. Makimoto, "Miniaturized hairpin resonator filters and their application to receiver front-end MIC'S," *IEEE Trans. Microwave Theory Tech.*, Vol. 37, No. 12, pp. 1991-1997, December 1989.

[3] S. Y. Lee and C. M. Tsai " New cross-coupled filter design using improved hairpin resonators," *IEEE Trans. Microwave Theory Tech.*, Vol. 48, No. 12, pp. 2482-2490, December 2000.

[4] A. Enokihara, K. Setsune, M. Sagawa, and M. Makimoto, " High-T/sub C/ bandpass filter using miniaturized microstrip hairpin resonator," *Electron. Lett.*, Vol. 28, No. 20, pp. 1925-1927, September 1992.

[5] D. Ahn, J. S. Park, C. S. Kim, J. Kim, Y. Qian, and T. Itoh, "A design of the lowpass filter using the novel microstrip defected ground structure," *IEEE Trans. Microwave Theory Tech.*, Vol. 49, No. 1, pp. 86-92, January 2001.

[6] J. W. Sheen," A compact semi-lumped low-pass filter for harmonics and spurious suppression," *IEEE Microwave and Guided Wave Lett.*, Vol. 10, No. 3, pp. 92-93, March 2000.

[7] L. -H. Hsieh and K. Chang, " Compact lowpass filter using stepped impedance hairpin resonator," *Electron. Lett.*, Vol. 37, No. 14, pp. 899-900, July 2001.

[8] L. -H. Hsieh and K. Chang, " Compact elliptic-function lowpass filters using microstrip stepped impedance hairpin resonators, " *IEEE Trans. Microwave Theory Tech.*, Vol. 51, No. 1, pp. 193-199, January 2003.

[9] F. Giannini, M. Salerno and R. Sorrention, "Design of low-pass elliptic filters by means of cascaded microstrip rectangular elements," *IEEE Trans. Microwave Theory Tech.*, Vol. 30, No. 9, pp. 1348-1353, September 1982.

[10] B. C. Wadell, *Transmission Line Design Handbook*, Norwood: Artech House, 1991, pp.320-321.

[11] P. R. Geffe, *Simplified Modern Filter Design*, New York: John F. Rider, 1963, Appendix 4.

[12] R. J. Wenzel, "Small elliptic-function low-pass filters and other applications of microwave C sections," *IEEE Trans. Microwave Theory Tech.*, Vol. 18, No. 12, pp. 1150-1158, December 1970.

[13] IE3D Version 8.0, Zeland Software Inc., Fremont, CA, January 2001.